*Biochimica et Biophysica Acta*, 1062 (1991) 103–107

*ADONIS* 000527369100102P



BBAMEM 70672

**BBA Report**

# Core-coat conductor of lipid bilayer and micromachined silicon

Peter Fromherz and Jürgen Klingler

*Abteilung Biophysik der Universität Ulm, Ulm-Eselsberg (F.R.G.)*

(Received 11 July 1990)

Key words: Model membrane; Membrane potential; Cable equation; Glycerol monooleate; Gramicidin; Silicon; Micromechanics

**We have etched a groove into a (110) plane of silicon and have covered it with a bilayer of glycerol monooleate. We have varied the depth of the groove, the concentration of salt in the electrolyte and the density of gramicidin in the membrane. We have clamped one end of the groove at a constant voltage with respect to the bath keeping the other end sealed or electrically open with respect to the bath. We have measured (i) the voltage at the center of the groove and at the sealed distal end and (ii) the current through the system in sealed and open configuration. We have found that the spread of voltage is in quantitative agreement with the stationary solutions of Kelvin's equation for a homogeneous cable.**

Important features of biomembranes are related to lateral spread of electrical voltage as in the case of action potentials in neural axons [1], of signal processing in neural dendrites [2,3] and of pattern formation in fluid membranes [4,5]. The simplest system where such processes may occur is a cable as described by Kelvin's equation for the one-dimensional core-coat conductor. The availability of a model system is crucial to study experimentally phenomena of spatio-temporal dynamics in membranes.

As a suitable geometry we have suggested the 'planar cable' as formed by a shallow groove in an isolating material – forming the core – which is covered by a planar membrane – forming the coat (Fig. 1). [6]. We have shown that a groove in a glass plate as covered by a black lipid membrane with ion channels exhibits all features of such a planar cable. A drawback of that set-up was, however, its difficult fabrication. The availability of planar cables of precise, reproducible geometry – narrow, shallow and branched – is a prerequisite for modelling signal processing and selforganization in neurites.

In the present paper we demonstrate that such planar cables may be produced on silicon wafers using the technology of micromachining. We investigate the spread of voltage at various depths of the cable, at various concentrations of electrolyte and at various densities of ion channels. The novel approach opens the route towards miniaturized, structured cables.

At first we summarize the relations describing electrotonic spread in a cable. Then we describe the experimental technique. Finally we present our measurements of voltage and current and evaluate the data in terms of the cable equation.

*Cable equation.* We consider a cable of length $l_M$, of a resistance $R_1$ per unit length of the internal conductor and of a conductance $G_M$ per unit length of the membrane (Fig. 1). A constant voltage $V_0$ is applied to one end (coordinate $x = 0$). The stationary voltage profile $V_M(x)$ is derived from Kelvin's cable equation [7]. For the configurations of sealed and open end ($x = l_M$) we obtain Eqn. 1 and Eqn. 2, respectively. The length constant is $\lambda = (R_1 \cdot G_M)^{-1/2}$.

$$V_M^{SE}(x) = V_0 \cdot \frac{\cosh[(l_M - x)/\lambda]}{\cosh(l_M/\lambda)} \quad (1)$$

$$V_M^{OE}(x) = V_0 \cdot \frac{\sinh[(l_M - x)/\lambda]}{\sinh(l_M/\lambda)} \quad (2)$$

Eqn. 1 defines the voltage at the sealed end $V_M^{SE}(l_M) = V_{SE}$ according to Eqn. 3. Integration of Eqns. 1 and 2 provides the total currents $I_{SE}$ and $I_{OE}$ through a sealed and open cable according to Eqns. 4 and 5. The input conductance of a semi-infinite cable is $G_\infty = (R_1/G_M)^{-1/2}$.

Correspondence: P. Fromherz, Abteilung Biophysik der Universität Ulm, D-7900 Ulm-Eselsberg, F.R.G.

$$V_{SE}/V_0 = 1/\cosh(l_M/\lambda) \quad (3)$$

$$I_{SE}/V_0 = G_\infty \cdot \mathrm{tgh}(l_M/\lambda) \quad (4)$$

$$I_{OE}/V_0 = G_\infty/\mathrm{tgh}(l_M/\lambda) \quad (5)$$

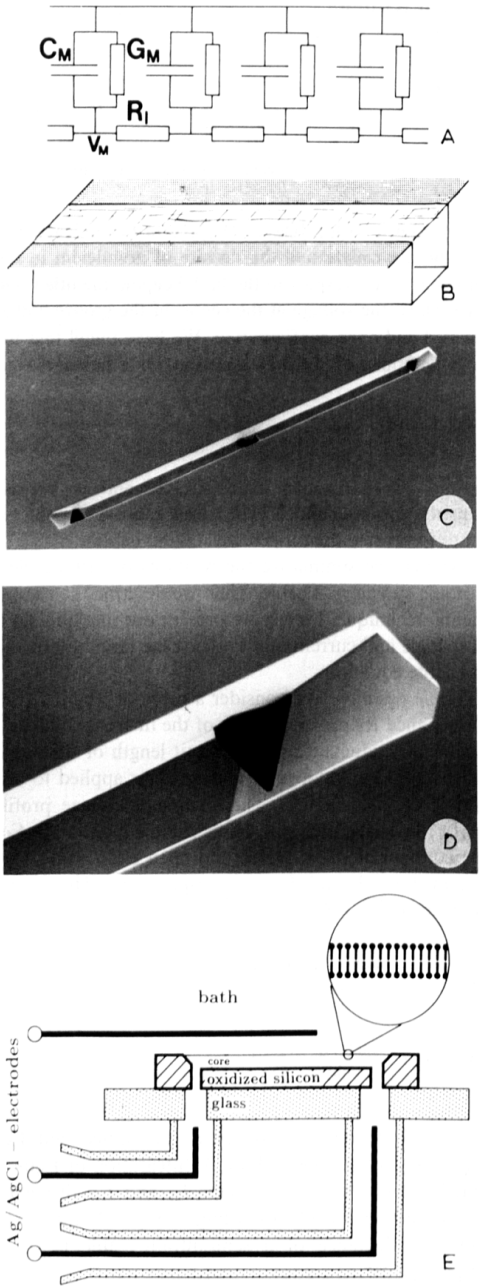


Combination of Eqns. 3, 4 and 5 leads to a parameter-free relation of the observable quantities $V_0$, $V_{SE}$, $I_{SE}$ and $I_{OE}$ according to Eqn. 6.

$$(V_{SE}/V_0)^2 = 1 - I_{SE}/I_{OE} \quad (6)$$

*Planar cable.* The geometry of a planar cable is defined by the length $l_M$ and the width $w_M$ of the membrane and by the depth $d_S$ of the subphase (Fig. 1). The core resistance is $R_I = (w_M \cdot d_S \cdot \Lambda_E \cdot [E])^{-1}$ if the specific resistance of the electrolyte is expressed by its molar concentration [E] and conductivity $\Lambda_E$. The coat conductance is $G_M = w_M \cdot n_{CH} \cdot \Lambda'_{CH} \cdot [E]$ if the specific conductivity of the membrane is expressed by the density $n_{CH}$ of ion channels and their conductance $\Lambda'_{CH} \cdot [E]$ which is proportional to the concentration of electrolyte. From these expressions for $R_I$ and $G_M$ we obtain Eqn. 7. The length constant $\lambda$ depends on the depth of the subphase and on the channel density. The width of the membrane and the concentration of electrolyte have no effect.

$$\lambda = \sqrt{d_S \cdot \Lambda_E/\Lambda'_{CH} \cdot n_{CH}} \quad (7)$$

Experimentally we may control depth and width of the cable and the concentration of electrolyte. We have no tool to determine directly the channel density. We evaluate it from the experimental currents in sealed and open configuration. With $n_{CH} = G_M/w_M \cdot \Lambda'_{CH} \cdot [E]$ and $G_M = G_\infty/\Lambda$ we obtain Eqn. 8 where $G_\infty$ and $\Lambda$ are expressed by Eqns. 9 and 10 as derived from Eqns. 4 and 5.

$$n_{CH} = \frac{G_\infty}{\lambda} \cdot \frac{1}{w_M \cdot \lambda'_{CH} \cdot [E]} \quad (8)$$

$$G_\infty = \sqrt{I_{SE} \cdot I_{OE}}/V_0 \quad (9)$$

$$\lambda = l_M/\mathrm{artgh}\sqrt{I_{SE}/I_{OE}} \quad (10)$$

*Silicon cell.* We use CZ-silicon wafers of a diameter of 100 nm, a thickness of 0.525 mm and a specific

Fig. 1. Planar Cable. (A) Equivalent circuit with resistance $R_I$ per unit length of the core and with conductance $G_M$ and capacitance $C_M$ per unit length of the coat. (B) A groove in an isolating support is filled with electrolyte and separated from bulk electrolyte by a planar lipid bilayer. (C) Scanning electronmicrograph of a groove in a silicon wafer (depth 170 $\mu$m, width 150 $\mu$m, length 3.9 mm) with three contacts from the back. (D) Details of the groove at one end. The bottom is formed by a (110) plane of silicon, the vertical and inclined walls are formed by three different (111) planes. The perforation from the back is etched along a (111) plane. (E) Schematic cross section of the whole cell.

resistance of 25 Ω cm (p-boron-doped) with a polished (110) surface (Wacker-Chemie/Burghausen). We cut them along two (111) planes into parallelograms of 10 mm × 25 mm using a diamond knife. We clean the plates by methanol, aceton, chloroform, aceton and methanol, sonicate with pure water (Milli-Q-system) and dry by centrifugation. We grow thermal silicon oxide in wet oxygen at 1000 °C in an oven (Heraeus/Hanau) [8]. The thickness (300 nm) is checked by reflection measurement. We apply a positive photoresist (AZ-1514, Hoechst/Frankfurt) to the polished surface by spin-coating. After prebaking at 90 °C for 20 min a strip mask is imaged onto the plate as alligned parallel to a (111) plane. After dissolution of the illuminated resist (AZ-developer) and postbaking at 130 °C for 45 min we etch the oxide by buffered 40% HF (Merck/Darmstadt). After removal of the photoresist by aceton we etch the exposed silicon by EDP-solution (1 l ethylenediamine, 160 g pyrocatechol, 6 g pyrazine, 133 g water) at 110 °C [9–11]. A groove is formed. Its walls are (111) planes, its bottom is a (110) plane (Fig. 1). The oxide is removed by HF. The depth of the grooves is evaluated from the conductivity of grooves filled with electrolyte and checked by direct measurement in some broken samples.

Another layer of thermal oxide (300 nm) is grown all over the plate. Photoresist is applied to the rough back and prebaked. A mask is imaged onto the back with short stripes (two or three) which are alligned along a (111) plane and which cross the ends of the groove and eventually its center. We dissolve the illuminated resist, postbake it and etch the exposed oxide by HF. After removal of the photoresist we etch the silicon by EDP-solution from the back until contact to the groove is attained. Finally a layer of thermal oxide of a thickness of 1.3 μm is grown all over the sample. At a temperature of 300 °C the plate is sintered with its back onto slide of duran-glass (30 mm × 15 mm × 2 mm) with borings applied at the locations of the groove contacts. Short glass tubes are molten to the back as connected to NS5-fittings (Fig. 1).

We clean the cell with cold chromic acid (Merck/Darmstadt) for 24 h and rinse with water. We coat the surface with octadecyl-trichlorosilane (OTS, Fluka/Neu-Ulm) [12] applied as a 2 vol% solution in chloroform/$CCl_4$ (vol. ratio 4:1) for 10–15 min and rinse with chloroform, methanol and water. We remove the silane in the groove by chromic acid. A coated cell is reused after cleaning with water, methanol, chloroform, methanol and water.

*Membrane and circuit.* We dip the cell into a beaker (volume 100 ml, surface 30 $cm^2$) filled with solutions of NaCl (Merck, Suprapure, kept for 6 h at 600 °C in an oven). Ag/AgCl electrodes are inserted into the NS5-joints and into the bath. We apply 100 μl of a 10 mM solution of glycerol monooleate (Sigma/Heidelberg) in decane (Merck) and 1–5 μl of a 500 ng/ml solution of gramicidin D (Sigma) in methanol to the air/water interface. The system is homogenized by dipping the cell in and out several times. After 10 min a membrane is formed by dipping, lifting and dipping the cell [13–16]. The lifetime of the black lipid membrane varies from 3 to 200 min.

We apply a DC-voltage of 15–50 mV to one end of the groove. The distal end is connected to a voltage-follower (operational amplifier TL 071, input resistance > 1 GΩ) (voltage at sealed end) or it is kept at bath potential (open end). The bath electrode is connected to a current/voltage converter (operational amplifier OPA 121) and kept on virtual ground (currents for open and sealed configuration). The applied voltage and the outputs of voltage-follower and current/voltage converter are read into a microcomputer (Apple II, 12-bit AD-converter) which switches between the condition of sealed and open end. The voltage clamp is exchanged repeatedly between the two ends of the groove to check for symmetry. In some cases the voltage is read from the central contact.

*Signal transmission.* We have used grooves of depths $d_S = 95$ μm and $d_S = 170$ μm at a width of $w_M = 150$ μm and a length of $l_M = 3.9$ mm. With both types of grooves we have used three concentrations of sodium chloride as [E] = 30 mM, 100 mM and 300 mM. With all six combinations we have prepared membranes with a variable amount of gramicidin.

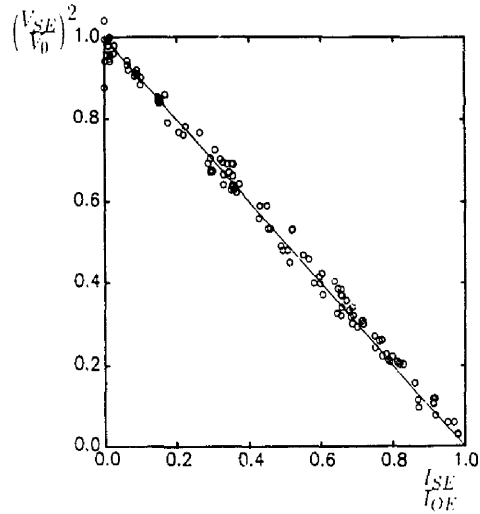


Fig. 2. Square of the ratio $V_{SE}/V_0$ of the voltage at sealed distal end and of the applied voltage versus the ratio $I_{SE}/I_{OE}$ of the currents through cable with sealed and open end. The data refer to cable depths of 95 μm and 170 μm and to NaCl concentrations of 30 mM, 100 mM and 300 mM at variable densities of gramicidin. The theoretical line is drawn according to Eqn. 6.

We have applied a constant voltage $V_0$ to one end of the cable. We have measured the voltage $V_{SE}$ at the end of a sealed cable and the currents $I_{SE}$ and $I_{OE}$ through the cable in sealed and open configuration. We have plotted the square of the voltage drop $V_{SE}/V_0$ versus the ratio of currents $I_{SE}/I_{OE}$ in Fig. 2 for all experiments with the two geometries and three salt concentrations. The data points are concentrated along a line of slope $-1$ which crosses ordinate and abscissa at $+1$. This result is in perfect agreement with the theoretical prediction for a homogeneous cable (Eqn. 6).

We replot the data to reveal the modulation of the length constant by the depth of the groove, by the concentration of electrolyte and by the density of channels. We evaluate the channel density $n_{CH}$ from the currents $I_{SE}$ and $I_{OE}$ according to Eqns. 8, 9 and 10. We evaluate the length constant $\lambda$ from the voltage drop $V_{SE}/V_0$ according to Eqn. 3. In the double logarithmic plot of $\lambda$ versus $n_{CH}$ (Fig. 3) the data are concentrated along two lines of slope $-1/2$. Thus the length constant drops with the reciprocal square root of the channel density. The data for the deep cable (170 $\mu$m) are shiften with respect to the data for the shallow cable (95 $\mu$m). The electrolyte concentration has no effect. Theoretical relations as obtained from Eqn. 7 with $\Lambda_E = 111$ S cm$^2$ mol$^{-1}$ and $\Lambda'_{CH} = 34$ pS/M (cf. Ref. 6) are plotted in Fig. 3. Experiment and theory are in perfect agreement.

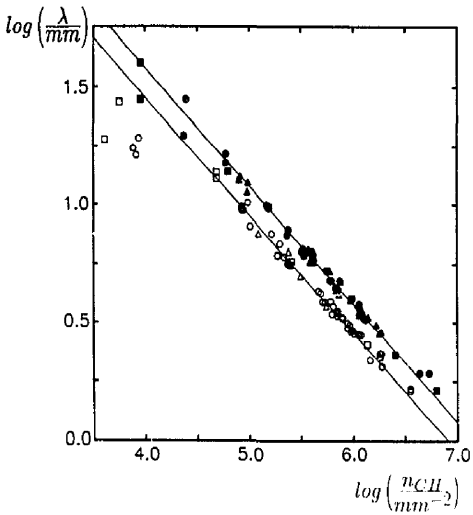


Fig. 3. Length constant $\lambda$ versus channel density $n_{CH}$. $\lambda$ is evaluated from the ratio $V_{SE}/V_0$ of the voltage at sealed end and of the applied voltage (Eqn. 3). $n_{CH}$ is evaluated from the currents $I_{SE}$ and $I_{OE}$ through the cable with sealed and open end (Eqns. 8, 9 and 10). Full symbols refer to a cable of 170 $\mu$m depth, open symbols refer to a cable depth of 95 $\mu$m. Triangles, circles and squares refer to NaCl concentrations of 30 mM, 100 mM and 300 mM, respectively. The theoretical lines are drawn according to Eqn. 7.

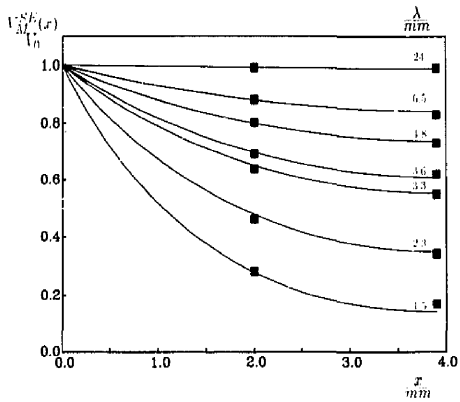


Fig. 4. Ratio $V_M^{SE}/V_0$ of voltage in a cable with sealed end and of applied voltage versus distance $x$ from the site of voltage clamp. Depth 170 $\mu$m, width 150 $\mu$m, length 3.9 mm, NaCl concentration 100 mM. The length constants $\lambda$ are evaluated from the ratio $I_{SE}/I_{OE}$ of the currents with sealed and open end (Eqn. 10). The theoretical curves are drawn according to Eqn. 1.

*Potential profile.* We have studied grooves of depth $d_S = 170$ $\mu$m, width $w_M = 150$ $\mu$m and length $l_M = 3.9$ mm with an additional contact in the center. We have measured the voltage at the center ($x = 2$ mm) and at the sealed end ($x = 3.9$ mm) and the currents $I_{SE}$ and $I_{OE}$ in sealed and open configuration. The voltages $V_M^{SE}(x)$ are plotted in Fig. 4 versus the distance $x$ for seven length constants $\lambda$ as evaluated from the currents according to Eqn. 10.

The voltage drop is steeper in the first part of the cable than in the second part. This inhomogeneity of the slope is more pronounced in cables with a large amount of added gramicidin. Theoretical relations of the voltage profile as obtained from Eqn. 1 are plotted in Fig. 4. Theory and experiment are in perfect agreement.

*Conclusion.* The combination of the BLM-technique with silicon technology provides well defined planar membrane cables. The set-up is suitable to study experimentally biophysical processes in membranes with spatio-temporal dynamics, in particular such processes where the membrane potential is coupled to lateral transport. Further developments must be directed towards an integration of the electrical contacts and towards detection of the spatial pattern of voltage as well as of lipid and protein at a high resolution.

This work was possible only on the background of the silicon technology as set up in our laboratory during the last few years by A. Offenhäusser, M. Brandstätter, V. Tegeder, F. Jäger and S. Jäger. We thank in particular Dr. A. Offenhäusser for his help in the initial steps of this work. We thank Dr. L. Csepregi/München for information about the EDP-technique. We thank Wacker-Chemie/Burghausen for a gift of silicon wafers.

The work was supported generously by the Fonds der Chemischen Industrie, by the Land Baden-Württemberg (Forschungsschwerpunkt 24) and by the Deutsche Forschungsgemeinschaft (grant Fr 349/5).

## References


1 Hodgkin, A.L. and Huxley, A.F. (1952) J. Physiol. (London) 117, 500–544.
2 Rall, W. and Rinzel, J. (1973) Biophys. J. 13, 648–688.
3 Koch, C., Poggio, T. and Torre, V. (1982) Philos. Trans. R. Soc. (London) B 298, 227–264.
4 Fromherz, P. (1988) Proc. Natl. Acad. Sci. USA 85, 6353–6357.
5 Fromherz, P. (1989) Biochim. Biophys. Acta 986, 341–345
6 Fromherz, P. and Klingler, J. (1989) Biochim. Biophys. Acta 987, 222–230.
7 Jack, J.J.B., Noble, D. and Tsien, R.W. (1985) Electrical current flow in excitable cells, Clarendon Press, Oxford.
8 Ong, D.G. (1984) Modern MOS Technology, McGraw Hill, New York.
9 Peterson, E. (1982) Proc. IEEE 70, 420–457.
10 Heuberger, A. (ed.) (1989) Mikromechanik, Springer, Berlin.
11 Csepregi, L. (1985) Microelectronic Eng. 3, 221–234.
12 Sagiv, J. (1980) J. Am. Chem. Soc. 102, 92–98.
13 Mueller, P., Rudin, D.O., Tien, H.T. and Wescott, W.C. (1962) Nature 194, 979–980.
14 Hanai, T., Haydon, D.A. and Taylor, J. (1964) Proc. Roy. Soc. (London) Ser. A 281, 377–391.
15 Vodyanoy, V. and Murphy, R.B. (1982) Biochim. Biophys. Acta 687, 189–194.
16 Dambacher, K.H. and Fromherz, P. (1986) Biochim. Biophys. Acta 861, 331–336.